JOURNAL OF
CLINICAL PRACTICE & RESEARCH

J Clin Pract Res 2023; 45(3): 248–52 • DOI: 10.14744/etd.2023.35306
ORIGINAL ARTICLE – OPEN ACCESS

Comparison of T2W FLAIR Images of Patients with Multiple Sclerosis and Ischemic Gliosis via Histogram Analysis

Murat Baykara[1], Mustafa Yıldırım[2], İsmail Taşkent[3], Hanefi Yıldırım[1], Duran Tavut[2]

Objective: In some cases, it may be challenging to differentiate radiologically between ischemic gliotic foci and multiple sclerosis (MS) plaques. This study aims to evaluate the effectiveness of histogram analysis in the differentiation of MS plaque and ischemic gliosis lesions on the T2-weighted (T2WI) FLAIR sequence.

Materials and Methods: This study was conducted on the Magnetic Resonance Imaging (MRI) examinations of patients diagnosed with ischemic gliosis and multiple sclerosis. Inactive lesions of 43 patients with ischemic gliosis and 46 with multiple sclerosis imaged by the same device were included in the study. Histogram analysis parameters of both groups were calculated. The entire image analysis algorithm was obtained through in-house software coded in MATLAB. Both groups were compared using a student's t-test. The diagnostic value of the parameters was detected with the receiver operating characteristic (ROC) curve.

Results: Mean gray level intensity, the standard deviation of the histogram, and entropy values calculated via minimum, maximum and median values were significantly higher in patients with ischemic gliosis. ROC curve analysis indicated that a threshold value of 545.19 for mean gray level intensity has 69.8% specificity and 69.6% sensitivity.

Conclusion: Histogram analysis may help differentiate MS and ischemic gliosis.

Keywords: Multiple Sclerosis; gliosis, ımage processing, histogram analysis, MRI

Cite this article as:
Baykara M, Yıldırım M, Taşkent İ, Yıldırım H, Tavut D. Comparison of T2W FLAIR Images of Patients with Multiple Sclerosis and Ischemic Gliosis via Histogram Analysis. J Clin Pract Res 2023; 45(3): 248-52.

[1]Department of Radiology, Fırat University Faculty of Medicine, Elazığ, Türkiye
[2]Department of Radilogy, University of Health Sciences, Elazığ Fethi Sekin City Hospital, Elazığ, Türkiye
[3]Department of Radiology, Muş State Hospital, Muş, Türkiye

Submitted
09.05.2022

Revised
26.08.2022

Accepted
07.03.2023

Available Online
13.04.2023

Correspondence
Mustafa Yıldırım, University of Health Sciences, Elazığ Fethi Sekin City Hospital, Department of Radilogy, Elazığ, Türkiye
Phone: +90 530 343 74 63
e-mail: mustafa23468@outlook.com

INTRODUCTION

Multiple sclerosis (MS) is an inflammatory, chronic, and degenerative neurological disease that causes physical and psychiatric problems such as weakness, loss of vision, bowel dysfunction, fatigue, mood symptoms, cognitive problems, depression, and anxiety (1). It is usually characterized by recurrent immune-mediated demyelination, glial scar formation, and axonal loss (1, 2).

Magnetic resonance imaging (MRI) is very successful in detecting intracranial and spinal abnormalities in patients with multiple sclerosis, including white matter damage observed through fluid-attenuated inversion recovery (FLAIR) sequence (3). Commonly, characteristic lesion morphology, distribution of lesions, and involvement of specific anatomical structures support the diagnosis of MS. However, it is essential to consider that several other disorders appear similarly in MRI with MS, especially in T2WI/FLAIR images (3).

In this respect, differentiating MS from acquired small vessel disease (SVD) on MRI images becomes a significant challenge due to the high prevalence of hypoxic/ischemic SVD leukoencephalopathy, commonly in middle-aged or elderly patients (3). SVD is a pathological process that affects perforating capillaries, cerebral arterioles, and venules (4). MS plaques are observed as multiple focal hyperintense lesions on the FLAIR sequence on MRI (3). Hypoxic/ischemic neurological damage is commonly caused by diseases that affect large or small blood vessels. The appearance of SVD in MRI is rarely interpreted as suggesting MS (3).

Digital images are used in radiologic practice. Small rectangular blocks or pixels (image elements) compose a two-dimensional digital image. Each pixel is represented through a set of coordinates in space and has a value to represent the gray-level intensity of a visual or volume in space. A texture of a digital image can be linked to the image's gray-level distribution. Texture characteristics are mathematical parameters calculated based on the pixel distribution characterizing the texture type, hence the basic structure of matters presented in the image (5).

Lesion heterogeneity may be helpful in the differential diagnosis of visually similar lesions. Texture analysis is used to assess lesion heterogeneity. Different texture parameters are used for this purpose. Entropy is one of the texture parameters recognized to measure homogeneity within the region of interest (ROI) (6, 7). It is the measure of changes in gray level and indicates inhomogeneity. It is defined as zero once all data are identical, and its value increases based on the irregularities in distribution (7, 8).

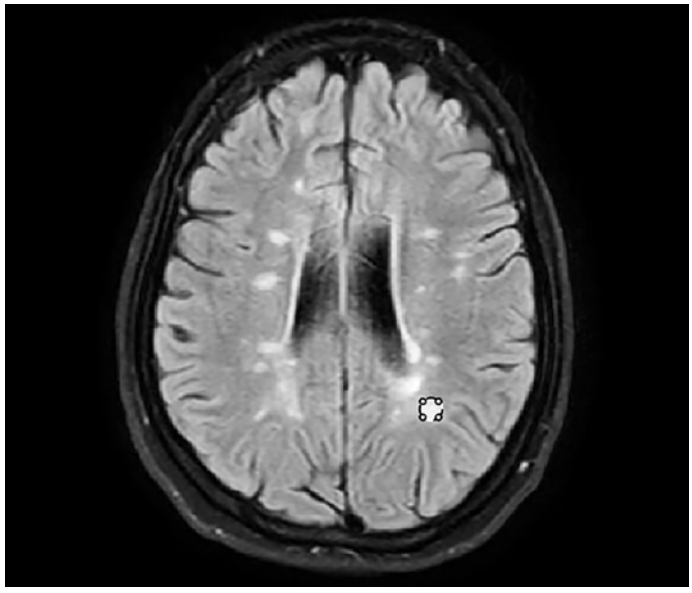

Figure 1. Histogram analysis for MS lesion on T2 FLAIR

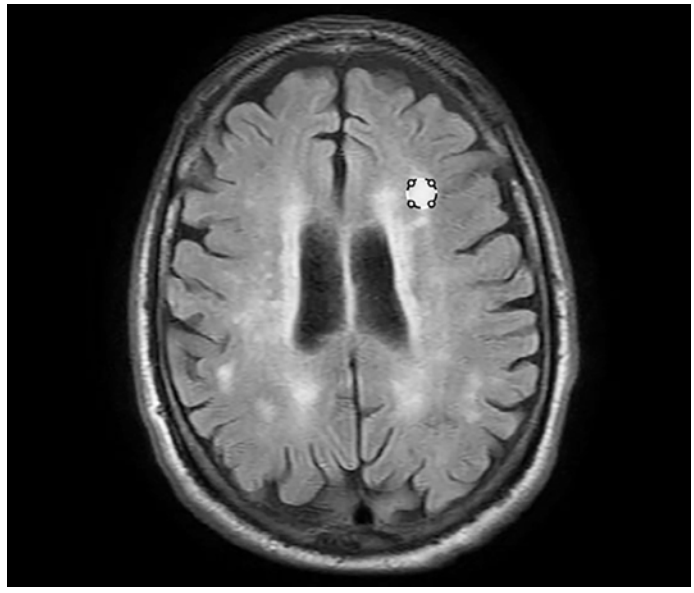

Figure 2. Histogram analysis for ischemic gliosis on T2 FLAIR

Uniformity refers to the closeness to the normal distribution of the gray level intensity of the image, and higher values indicate a more normal distribution (7, 8). Skewness suggests asymmetry in distribution, with more values to the left of the mean indicating a positive skewness and the opposite indicating a negative skewness (8).

Kurtosis is the measure of the peak in distribution. Once the histogram has a bell curve, its value becomes three, and the histogram curve with a sharper peak has a more significant value than three (8). Size %lower, size %upper, and size %mean (%L, %U, and %M) indicate the areas in the histogram (9). These techniques recently attracted particular attention (5, 10, 11) and were used in various diagnoses, such as tumor characterization (12), prognostic biomarkers identification (13–16), and radiotherapy guidance (17).

MR histogram studies have been performed in patients with multiple sclerosis (18), and several parameters were compared; however, no study compared the MR histogram findings of MS and SVD. Cerebral small vessel disease causes ischemic gliotic focus. Ischemic gliotic foci are hyperintense white matter lesions on the T2W FLAIR image. In some cases, it may be challenging to differentiate radiologically between ischemic gliotic foci and MS plaques. This study aims to differentiate between MS plaque and SVD through the histogram analysis of T2W FLAIR sequence images.

MATERIALS and METHODS

Fırat University Ethics Committee approved this study (date: 05/07/2018, number: 12/01). Because the study is retrospective, patients' written informed permission could not be acquired. This retrospective study was conducted on the MRI examinations of patients diagnosed with ischemic gliosis and multiple sclerosis. Between 2020–2022 years, inactive lesions of 43 patients with ischemic gliosis and 46 with multiple sclerosis imaged by the same device were considered.

MS patients in Group 1 were diagnosed using the 2017 McDonald Criteria. Patients with MS were randomly selected from the hospital database. Only patients with the relapsing-remitting form of the disease were enrolled in the study. Other forms of MS were not included in the study.

Group 2 included patients with SVD. Patients with hyperintense areas on T2W FLAIR images consistent with SVD were included in the study (Fazekas grade=1–2) (19). Patients with SVD were randomly selected from the hospital database. Any cause of stroke other than SVD (such as a cardioembolic source or extra- or intracranial artery stenosis of >50%), any significant central nervous system illnesses (neurosarcoidosis, systemic lupus erythematosus, rheumatic arthritis, toxic, metabolic, infectious, metastatic diseases, dementia, and other vasculitis diseases), and significant psychiatric disorders were excluded.

The MRI examinations were conducted with a 1.5T Philips Ingenia device (Philips, Best, Netherlands). Images of axial FLAIR were transferred to an iMac PC (Apple Inc). The histogram analysis was performed with OsiriX V.4.9 image software (Pixmeo, Switzerland) utilizing the region of interest (ROI).

All lesions were selected from periventricular white matter. ROI was specified to cover 2/3 of the hyperintense lesion in sections (Fig. 1, 2). Histogram analysis parameters were calculated, and the entire image analysis algorithm was obtained through in-house software coded in MATLAB (version R2009b).

Statistical Analysis

The statistical analyses were conducted with IBM SPSS for Windows, version 22.0 (IBM Statistics, IBM Corporation, Armonk, New York, USA). The normality of the data distribution was analyzed with the Kolmogorov–Smirnov test. Student-t test was used for normally distributed data. Mann Whitney U test was used for non-normally distributed data. Statistical significance value was defined as a value of $p<0.05$. Mean±standard deviation was used in expressing the data. The post-power of the study was calculated with G*Power software (version 3.1.9.4). The discrimination performance of the parameters was determined using a ROC curve. The cut-off value was determined with the Youden index.

Table 1. Minimum, median, and maximum values of the parameters of both groups

	Ischemic gliosis (n=43)			Multiple sclerosis (n=46)		
	Median	**Minimum**	**Maximum**	**Median**	**Minimum**	**Maximum**
Mean	477.12	97.13	862.00	223.02	98.38	1004.09
Standard deviation	15.41	4.26	54.23	9.51	3.11	53.98
Minimum	439.00	72.00	793.00	194.00	83.00	893.00
Maximum	509.00	116.00	900.00	241.00	106.00	1090.00
Median	477.50	101.00	869.00	225.00	98.00	1004.50
Variance	237.60	18.12	2940.83	90.35	9.70	2913.96
Entropy	5.04	3.33	6.44	4.81	3.47	6.77
Size %L	15.75	9.09	25.00	16.04	5.00	27.27
Size %U	17.30	0.00	22.83	16.67	3.85	22.90
Size %M	67.26	56.25	83.87	67.77	59.09	82.35
Kurtosis	2.69	1.81	7.39	2.64	1.92	7.02
Skewness	-0.29	-2.12	0.63	-0.28	-1.73	0.94
Uniformity	0.39	0.17	0.68	0.38	0.21	0.60

L: Lower; U: Upper; M: Mean

Table 2. Distribution of the histogram analysis values based on groups

	Ischemic gliosis (n=43) Mean±SD	**Multiple sclerosis (n=46) Mean±SD**	**p***	**p****
Mean	**597.98±145.20**	**412.89±258.25**		**<0.001**
Standard deviation	**27.21±12.54**	**20.09±15.21**		**0.007**
Minimum	**529.37±126.89**	**362.39±225.15**		**<0.001**
Maximum	**648.09±155.53**	**454.13±287.25**		**<0.001**
Median	**599.33±146.81**	**413.20±258.27**		**<0.001**
Variance	**893.84±758.87**	**629.97±783.89**		**0.007**
Entropy	**5.57±0.60**	**5.11±0.89**	**0.005**	
Size %L	16.26±2.63	15.76±3.43	0.448	
Size %U	16.83±3.68	16.17±3.67		0.344
Size %M	66.90±4.69	68.06±5.29	0.278	
Kurtosis	2.79±0.71	2.95±0.93		0.673
Skewness	-0.275±0.465	-0.268±0.531		0.650
Uniformity	0.377±0.091	0.367±0.073	0.595	

*: Student t; **: Mann-Whitney U; SD: Standard deviation; L: Lower; U: Upper; M: Mean

RESULTS

The mean age of the patients with ischemic gliosis was higher (patients with ischemic gliosis and multiple sclerosis were 68.70±10.94 and 40.25±11.72 years, respectively; p<0.001). The post-hoc power was calculated as 85%. All parameters' median, minimum, and maximum values were determined (Table 1). Mean gray level intensity, a standard deviation of a histogram, and minimum, maximum, median, and entropy values were significantly higher in patients with ischemic gliosis (Table 2). A ROC curve was carried out for mean gray level intensity, and the area under the curve (AUC) was determined as 0.715. This AUC value was interpreted as fair (20). When the threshold value was 545.19, 69.8% specificity and 69.6% sensitivity were found in differentiating ischemic focus and MS plaque (Fig. 3). Using ROC analysis, the AUC value for entropy was 0.655. When the cut-off value was selected as 5.506 for entropy, ischemic focus, and MS plaque could be differentiated with a sensitivity of 73.9% and specificity of 62.8%.

DISCUSSION

MRI is a powerful instrument for MS diagnosis based on T2-weighted white matter lesions and for monitoring treatment response and disease activity in clinical practice (1). Typical MS le-

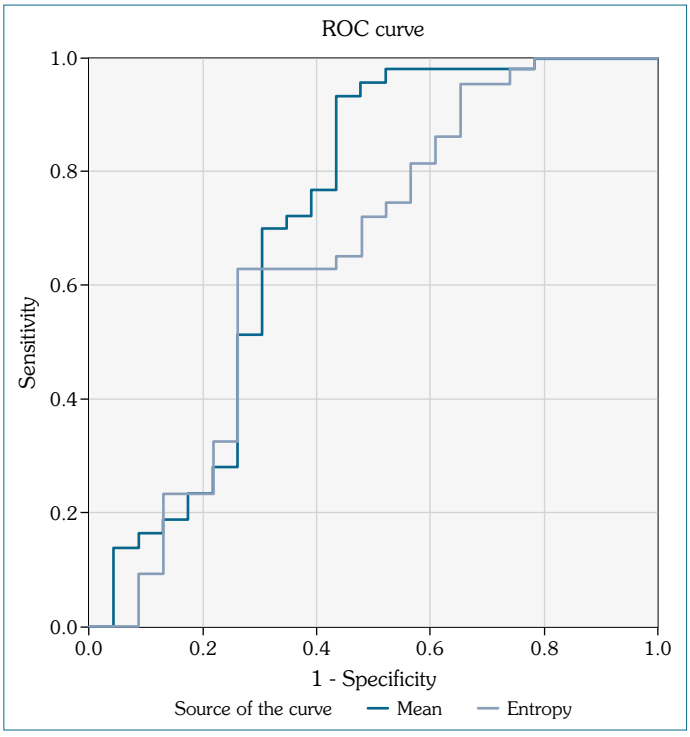

Figure 3. ROC curve graph for mean gray level intensity and entropy

sions are localized in periventricular, juxtacortical, and infratentorial brain areas. Multiple focal lesions with solid signals on T2-weighted imaging are usually seen. Lesions are commonly bilateral, and they are not generally symmetrical. However, overreliance on radiologic signs may lead to misdiagnosis of MS (21). Diseases misdiagnosed as MS are usually small vessel disease, idiopathic transverse myelitis, neuromyelitis optica spectrum disorder, and fibromyalgia (22).

A common radiological mimic of MS is small vessel disease. SVD can cause many focal hyperintensities in the subcortical white matter, similar to MS. But, unlike MS, these lesions spare the subcortical U-fibers and do not affect the corpus callosum or cerebellum (3). Despite all this, the radiological distinction between MS and SVD may be difficult in some cases. Our study aimed to demonstrate whether histogram analysis could help differentiate MS and SVD.

The present study established that the standard deviation and the entropy values calculated via the minimum, maximum, and median values were higher in patients with ischemic gliosis when compared to the MS patients (Table 1). Furthermore, the ROC curve analysis indicated that the AUC value for mean gray level intensity was 0.715. Once the threshold value was selected as 545.19, it was observed that 69.8% specificity and 69.6% sensitivity were available for differentiation. Loizou et al. (23) indicated a significant increase in mean and median parameters for the MS patient group compared to the control group. Our study found that SVD patients presented higher parameters when compared to MS patients. Such a finding stemmed from comparing the gliosis areas and the inactive MS lesions.

MRI and neuropathological studies have shown that active lesions contain severe inflammation, perivascular cuffing, monocyte infiltration, and loss of barrier. Disruption of the blood-brain barrier in active MS plaques is demonstrated using contrast-enhanced MRI (24, 25). Although the underlying causes of MS and SVD are not established, it is possible to state that the blood-brain barrier is disrupted in both diseases as a standard feature (26). The blood-brain barrier disruption is linked to entropy values (27). In our study, entropy was another statistically significant analysis parameter; entropy values of inactive MS lesions were lower compared to the secondarily developed gliotic foci in SVD. Hence, this parameter may be helpful in the differentiation of ischemic foci and MS plaques. Michoux et al. (27) detected a significant increase in entropy values in patients with lacunar infarction compared to cortical ischemia. Similarly, the present study indicated higher entropy values for small vessel disease.

Loizou et al. (18) found that parameters such as standard deviation, entropy, and variance significantly increased during MS episodes but decreased after 6–12 months. Similar studies (28) indicated higher entropy values in active MS lesions than those with inactive lesions. Such a finding was considered due to further disrupting the blood-brain in active MS lesions. In the present study, histogram analysis was carried out with inactive MS lesions. These findings can explain the lower entropy values in MS lesions compared to SVD in our study.

Although there are many histogram analysis studies on MS, a histogram analysis study on the distinction between MS and SVD could not be found in the literature. Tozer et al. (29) reported that central veins in white matter lesions could differentiate primary progressive MS from SVD (29). The present study used histogram analysis to differentiate relapsing-remitting MS from SVD. Central vein sign is a visual data. But histogram analysis provides numeric data.

Limitations

The study was conducted in a single center, and the number of cases was low. A single slice was used for histogram analysis. Histogram analysis with 3D imaging would more accurately reflect the entire lesion. The age and volume differences of the lesions may affect the histogram analysis results. In addition, the higher mean age of the ischemia group is another study limitation.

It is possible to consider obtaining histogram analyses in other studies from T1A images as a limitation. However, similar results were obtained from T1A and FLAIR sequences in SVD patients in a study conducted by Tozer et al. (29).

CONCLUSION

As a result, histogram analysis may help differentiate MS plaque and ischemic gliotic foci.

Ethics Committee Approval: The Fırat University Clinical Research Ethics Committee granted approval for this study (date: 05.07.2018, number: 12/01).

Informed Consent: Written informed consent was obtained from patients who participated in this study.

Peer-review: Externally peer-reviewed.

Author Contributions: Concept – MB, MY, İT; Design – MY, MB, HY; Supervision – HY, DT, MY; Resource – MB, İT, MY; Materials – MB, DT, HY; Data Collection and/or Processing – MB, DT; Analysis and/or Interpretation – MB, İT, MY; Literature Search – MB, MY; Writing – MB, MY, İT; Critical Reviews – MB.

Conflict of Interest: The authors have no conflict of interest to declare.

Financial Disclosure: The authors declared that this study has received no financial support.

REFERENCES

1. Zhou F, Zhuang Y, Gong H, Zhan J, Grossman M, Wang Z. Resting state brain entropy alterations in relapsing remitting multiple sclerosis. PloS one 2016; 11(1): e0146080.[CrossRef]
2. Rumzan R, Chen X, Li YM Gray matter involvement in patients with multiple sclerosis as shown by magnetic resonance imaging. Chinese Med J 2012; 125(13):2361–4.
3. Aliaga ES, Barkhof F. MRI mimics of multiple sclerosis. Handb Clin Neurol 2014; 122: 291–316. [CrossRef]
4. Wardlaw JM, Smith C, Dichgans M. Mechanisms of sporadic cerebral small vessel disease: insights from neuroimaging. Lancet Neurol 2013; 12(5): 483–97. [CrossRef]
5. Castellano G, Bonilha L, Li LM, Cendes F. Texture analysis of medical images. Clin Radiol 2004; 59(12): 1061–9. [CrossRef]
6. Yu H, Caldwell C, Mah K, Poon I, Balogh J, MacKenzie R, et al. Automated radiation targeting in head-and-neck cancer using region-based texture analysis of PET and CT images. Int J Radiat Oncol Biol Phys 2009; 75(2): 618–25. [CrossRef]
7. Ganeshan B, Miles KA, Young RC, Chatwin CR. Texture analysis in non-contrast enhanced CT: impact of malignancy on texture in apparently disease-free areas of the liver. Eur J Radiol 2009; 70(1): 101–10.
8. Suo ST, Zhuang ZG, Cao MQ, Qian LJ, Wang X, Gao RL, et al. Differentiation of pyogenic hepatic abscesses from malignant mimickers using multislice-based texture acquired from contrast-enhanced computed tomography. Hepatobiliary Pancreat Dis Int 2016; 15(4): 391–8.
9. Yamashita K, Yoshiura T, Hiwatashi A, Togao O, Kikuchi K, Inoguchi T, et al. The radiological diagnosis of fenestral otosclerosis: the utility of histogram analysis using multidetector row CT. Eur Arch Otorhinolaryngol 2014; 271(12): 3277–82. [CrossRef]
10. Yildirim M, Baykara M. Differentiation of progressive disease from pseudoprogression using MRI histogram analysis in patients with treated glioblastoma. Acta Neurol Belg 2022; 122(2): 363–8. [CrossRef]
11. Yildirim M, Baykara M. Differentiation of multiple myeloma and lytic bone metastases: histogram analysis. j Comput Assist Tomogr 2020; 44(6): 953–5. [CrossRef]
12. Ganeshan B, Abaleke S, Young RC, Chatwin CR, Miles KA. Texture analysis of non-small cell lung cancer on unenhanced computed tomography: initial evidence for a relationship with tumour glucose metabolism and stage. Cancer Imaging 2010; 10(1): 137–43. [CrossRef]
13. Ganeshan B, Panayiotou E, Burnand K, Dizdarevic S, Miles K. Tumour heterogeneity in non-small cell lung carcinoma assessed by CT texture analysis: a potential marker of survival. Eur Radiol 2012; 22(4): 796–802. [CrossRef]
14. Yang D, Rao G, Martinez J, Veeraraghavan A, Rao A. Evaluation of tumor-derived MRI-texture features for discrimination of molecular subtypes and prediction of 12-month survival status in glioblastoma. Med Phys 2015; 42(11): 6725–35. [CrossRef]
15. Tixier F, Hatt M, Le Rest CC, Le Pogam A, Corcos L, Visvikis D. Reproducibility of tumor uptake heterogeneity characterization through textural feature analysis in 18F-FDG PET. J Nucl Med 2012; 53(5): 693–700. [CrossRef]
16. Molina D, Pérez-Beteta J, Luque B, Arregui E, Calvo M, Borrás JM, et al. Tumour heterogeneity in glioblastoma assessed by MRI texture analysis: a potential marker of survival. Br J Radiol 2016; 89(1064): 20160242. [CrossRef]
17. Lambin P, Petit SF, Aerts HJ, van Elmpt WJ, Oberije CJ, Starmans MH, et al. The ESTRO Breur Lecture 2009. From population to voxel-based radiotherapy: exploiting intra-tumour and intra-organ heterogeneity for advanced treatment of non-small cell lung cancer. Radiother Oncol 2010; 96(2): 145–52. [CrossRef]
18. Loizou CP, Petroudi S, Seimenis I, Pantziaris M, Pattichis CS. Quantitative texture analysis of brain white matter lesions derived from T2-weighted MR images in MS patients with clinically isolated syndrome. J Neuroradiol 2015; 42(2): 99–114. [CrossRef]
19. Fazekas F, Kleinert R, Offenbacher H, Schmidt R, Kleinert G, Payer F, et al. Pathologic correlates of incidental MRI white matter signal hyperintensities. Neurology 1993; 43(9): 1683–89. [CrossRef]
20. Safari S, Baratloo A, Elfil M, Negida A. Evidence based emergency medicine; Part 5 receiver operating curve and area under the curve. Emergency 2016; 4(2): 111–3.
21. Barkhof F, Filippi M, Miller DH, Scheltens P, Campi A, Polman CH, et al. Comparison of MRI criteria at first presentation to predict conversion to clinically definite multiple sclerosis. Brain 1997; 120(Pt 11): 2059–69. [CrossRef]
22. Thompson AJ, Banwell BL, Barkhof F, Carroll WM, Coetzee T, Comi G, et al. Diagnosis of multiple sclerosis: 2017 revisions of the McDonald criteria. Lancet Neurol 2018; 17(2): 162–73. [CrossRef]
23. Loizou CP, Murray V, Pattichis MS, Seimenis I, Pantziaris M, Pattichis CS. Multiscale amplitude-modulation frequency-modulation (AM-FM) texture analysis of multiple sclerosis in brain MRI images. IEEE Trans Inf Technol Biomed 2011; 15(1): 119–29. [CrossRef]
24. Ortiz GG, Pacheco-Moisés FP, Macías-Islas MÁ, Flores-Alvarado LJ, Mireles-Ramírez MA, González-Renovato ED, et al. Role of the blood-brain barrier in multiple sclerosis. Arch Med Res 2014; 45(8): 687–97.
25. Wardlaw JM, Makin SJ, Valdés Hernández MC, Armitage PA, Heye AK, Chappell FM, et al. Blood-brain barrier failure as a core mechanism in cerebral small vessel disease and dementia: evidence from a cohort study. Alzheimers Dement 2017; 13(6): 634–43. [CrossRef]
26. Valdés Hernández MDC, González-Castro V, Chappell FM, Sakka E, Makin S, Armitage PA, et al. Application of texture analysis to study small vessel disease and blood-brain barrier integrity. Front Neurol 2017; 8: 327. [CrossRef]
27. Michoux N, Guillet A, Rommel D, Mazzamuto G, Sindic C, Duprez T. Texture analysis of T2-weighted MR images to assess acute inflammation in brain MS lesions. PLoS One 2015; 10(12): e0145497. [CrossRef]
28. Samaraweera APR, Falah Y, Pitiot A, Dineen RA, Morgan PS, Evangelou N. The MRI central vein marker; differentiating PPMS from RRMS and ischemic SVD. Neurol Neuroimmunol Neuroinflamm 2018; 5(6): e496. [CrossRef]
29. Tozer DJ, Zeestraten E, Lawrence AJ, Barrick TR, Markus HS. Texture analysis of T1-weighted and fluid-attenuated inversion recovery images detects abnormalities that correlate with cognitive decline in small vessel disease. Stroke 2018; 49(7): 1656–61. [CrossRef]